Research Article | Vol. 25, No. 24 | 27 Nov 2017 | OPTICS EXPRESS 30780

Optics EXPRESS

# Accurate measurements of circular and residual linear birefringences of spun fibers using binary polarization rotators

ZHEXI XU,[1,3,4,5] X. STEVE YAO,[2,6,*] ZHENYANG DING,[1,3,4,5,9] X. JAMES CHEN,[6] XIN ZHAO,[7] HAO XIAO,[8] TING FENG,[2] AND TIEGEN LIU[1,3,4,5]

[1]*College of Precision Instrument & Optoelectronics Engineering, Tianjin University, Tianjin 300072, China*
[2]*Optical Information Innovation Center, College of Physical Sciences and Technologies, Hebei University, Baoding, Hebei Province, China*
[3]*Institute of Optical Fiber Sensing of Tianjin University, Tianjin 300072, China*
[4]*Tianjin Optical Fiber Sensing Engineering Center,Tianjin 300072, China*
[5]*Key Laboratory of Optoelectronics Information Technology, Ministry of Education, Tianjin 300072, China*
[6]*General Photonics Corporation, California 91710, USA*
[7]*Suzhou Optoring Co. Limited, Jiangsu Province, 215123 China*
[8]*Beijing SWT Optical Intelligent Technology Co., Ltd, Beijing 065201,China*
[9]*zyding@tju.edu.cn*
[*]*steveyao888@yahoo.com*

**Abstract:** We present a method to accurately measure the birefringence properties of spun fibers using binary polarization rotators. By taking the advantages of binary polarization rotator in polarization analysis, we are able to simultaneously measure both the circular and linear birefringences in a spun fiber with high accuracy. We obtain the circular and the residual linear birefringences of the spun fiber as a function of temperature T to be $3.34 \times 10^{-5}$-$5.11 \times 10^{-8}$T and $8.1 \times 10^{-6}$-$1.19 \times 10^{-8}$T, respectively, with the residual linear birefringence about 4 times less than the circular birefringence. We find, for the first time with the best of authors' knowledge, that the circular and the residual linear birefringences in a spun fiber are highly linear with the temperature, with thermal coefficients of $-5.11 \times 10^{-8}$ °$C^{-1}$ and $-1.19 \times 10^{-8}$°$C^{-1}$, respectively, and that the relative changes per °C of the circular and residual linear birefringence are almost identical, with values of −0.152% and −0.147% respectively. We believe that the method and data presented in this paper will be beneficial for making high quality spun fibers, as well as high accuracy fiber optic current sensors.



**OCIS codes:** (060.2300) Fiber measurements; (060.2400) Fiber properties; (120.5410) Polarimetry; (260.1440) Birefringence;(060.2370) Fiber optics sensors.

## References and links

1. R. I. Laming and D. N. Payne, "Electric current sensors employing spun highly birefringent optical fibers," J. Lightwave Technol. **7**(12), 2084–2094 (1989).
2. I. G. Clarke, "Temperature-stable spun elliptical-core optical-fiber current transducer," Opt. Lett. **18**(2), 158–160 (1993).
3. N. Peng, Y. Huang, S. Wang, T. Wen, and W. Liu, "Fiber optic current sensor based on special spun highly birefringent fiber," IEEE Photonics Technol. Lett. **25**(17), 1668–1671 (2013).
4. L. Li, J. R. Qian, and D. N. Payne, "Current sensors using highly birefringent bow-tie fibres," Electron. Lett. **22**(21), 1142–1144 (1986).
5. D. Tang, A. H. Rose, G. W. Day, and S. M. Etzel, "Annealing of linear birefringence in single-mode fiber coils: application to optical fiber current sensors," J. Lightwave Technol. **9**(8), 1031–1037 (1991).
6. K. Bohnert, P. Gabus, J. Nehring, and H. Brandle, "Temperature and vibration insensitive fiber-optic current sensor," J. Lightwave Technol. **20**(2), 267–276 (2002).
7. K. Kurosawa, S. Yoshida, and K. Sakamoto, "Polarization properties of the flint glass fibre," J. Lightwave Technol. **13**(7), 1378–1384 (1995).

#308276 https://doi.org/10.1364/OE.25.030780
Journal © 2017 Received 29 Sep 2017; revised 30 Oct 2017; accepted 3 Nov 2017; published 22 Nov 2017

Optics EXPRESS

8. S. X. Short, J. U. De Arruda, A. A. Tselikov, and J. N. Blake, "Elimination of Birefringence Induced Scale Factor Errors in the In-Line Sagnac Interferometer Current Sensor," J. Lightwave Technol. **16**(10), 1844–1850 (1998).
9. Fibercore white paper, "Products and Services," (Fibercore, 2017), http://fibercore.com/product/spun-hibi-fiber.
10. International Standard, Instrument transformers – Part 8: Electronic current transformers (IEC 60044–8, 2002), Chap. 4. 2. 1, Chap. 12. 2.
11. State Grid Corporation of China, Performance testing programme of the electronic instrument transformer (2014), Chap. 4.
12. J. F. Lin, "Concurrent measurement of linear and circular birefringence using rotating-wave-plate Stokes polarimeter," Appl. Opt. **47**(25), 4529–4539 (2008).
13. D. H. Goldstein, "Mueller matrix dual-rotating retarder polarimeter," Appl. Opt. **31**(31), 6676–6683 (1992).
14. P. A. Williams, "Rotating-wave-plate Stokes polarimeter for differential group delay measurements of polarization-mode dispersion," Appl. Opt. **38**(31), 6508–6515 (1999).
15. E. Dijkstra, H. Meekes, and M. Kremers, "The high-accuracy universal polarimeter," J. Phys. D **24**(10), 1861–1868 (1991).
16. P. A. Williams, A. H. Rose, and C. M. Wang, "Rotating-polarizer polarimeter for accurate retardance measurement," Appl. Opt. **36**(25), 6466–6472 (1997).
17. F. Treviño-Martínez, D. Tentori, C. Ayala-díaz, and F. J. Mendieta-Jiménenz, "Birefringence assessment of single-mode optical fibers," Opt. Express **13**(7), 2556–2563 (2005).
18. D. Jamon, F. Royer, F. Parsy, E. Ghibaudo, and J. E. Broquin, "Birefringence Measurements in Optical Waveguides," J. Lightwave Technol. **31**(19), 3151–3157 (2013).
19. B. B. Wang, "Stokes polarimeter using two photoelastic modulators," Proc. SPIE **5531**, 367–374 (2002).
20. X. S. Yao, X. Chen, and T. Liu, "High accuracy polarization measurements using binary polarization rotators," Opt. Express **18**(7), 6667–6685 (2010).
21. X. S. Yao, X. Chen, and L. Yan, "Self-calibrating binary polarization analyzer," Opt. Lett. **31**(13), 1948–1950 (2006).
22. X. S. Yao, L. Yan, and Y. Shi, "Highly repeatable all solid-state polarization state generator," Opt. Lett. **30**(11), 1324–1326 (2005).
23. R. Ulrich, S. C. Rashleigh, and W. Eickhoff, "Bending-induced birefringence in single-mode fibers," Opt. Lett. **5**(6), 273–275 (1980).
24. S. Manhas, M. K. Swami, P. Buddhiwant, N. Ghosh, and P. K. Gupta, "Mueller matrix approach for determination of optical rotation in chiral turbid media in backscattering geometry," Opt. Express **14**(1), 190–202 (2006).
25. S. Y. Lu and R. A. Chipman, "Interpretation of Mueller matrices based on polar decomposition," J. Opt. Soc. Am. A **13**(5), 1106–1113 (1996).
26. P. Olivard, P. Y. Gerligand, B. L. Jeune, J. Cariou, and J. Lotrian, "Measurement of optical fibre parameters using an optical polarimeter and Stokes-Mueller formalism," J. Phys. D **32**(14), 1618–1625 (1999).
27. Z. Ding, Z. Meng, X. S. Yao, X. Chen, and T. Liu, "Accurate method for measuring the thermal coefficient of group birefringence of polarization-maintaining fibers," Opt. Lett. **36**(11), 2173–2175 (2011).
28. K. Mochizuki, Y. Namihira, and Y. Ejiri, "Birefringence variation with temperature in elliptically cladded single-mode fibers," Appl. Opt. **21**(23), 4223–4228 (1982).
29. Z. Li, X. S. Yao, X. Chen, H. Chen, and Z. Meng, "Complete characterization of polarization-maintaining fibers using distributed polarization analysis," J. Lightwave Technol. **33**(2), 372–380 (2015).

## 1. Introduction

Fiber optic current sensors (FOCS) based on Faraday effects for measuring the electric current in power systems have the advantages of inherent insulation, immunity to electromagnetic interference and light weight. Unfortunately, variations in stress and temperature of the sensing fiber may change the distribution of linear birefringence in the fiber, which alter the polarization of light in the fiber and degrade sensor system's measurement accuracy [1]. In order to reduce the influence of temperature and external stresses, it is desirable to make the sensing fiber with high circular birefringence or low linear birefringence, for example, the spun fiber [1–4], the annealed fiber [5,6], the low-stress fiber [7], or the helically wrapped fiber [8]. Among the various fibers, the spun fiber is better accepted in the industry [3] for its manufacturability and high sensing accuracy over a wide range of environmental conditions, including temperature and vibration, making it suitable for current sensors deployed in both indoors and outdoors in real-life applications.

A spun fiber can be fabricated by first making a preform with two stress rods similar to that for making a linear polarization maintaining fiber (e.g. a bow-tie fiber or a PANDA fiber), and then spinning the perform during drawing in the molten state [4]. The spinning process induces a large circular birefringence and significantly reduces the average linear

Optics EXPRESS

birefringence over distance, although the local linear birefringence still remains strong [4] to overcome the stress and temperature induced birefringence perturbations. It is important to have the detailed knowledge of the circular and the residual total linear birefringences of the spun fiber, particularly their temperature dependences, to ensure that the current sensing system incorporating the fiber is insensitive to temperature variations and external stresses and eventually meets its performance requirements.

In a commercial spun fiber's data sheet (e.g. Spun HiBi Fiber of Fibercore Ltd.) [9], a parameter called elliptical beat length (circular beat-length in [9]) is generally used to describe its birefringence characteristics, which is estimated using the linear beat length of the un-spun fiber made with the same perform and spin pitch of the spinning process [4]. Such parameters mainly come from the point of view of spun fibers' manufacturers and are indeed intuitive to the manufacturing engineers of the spun fibers, however, they only provide indirect descriptions of fibers' birefringence characteristics which are critical to the users of the spun fibers. Although the residual linear birefringence $\Delta n_L$ and circular birefringence $\Delta n_C$ of a spun fiber can be estimated by the parameters of the elliptical beat length and spin pitch in theory [1], the obtained $\Delta n_L$ and $\Delta n_C$ are usually significantly different from the actual $\Delta n_L$ and $\Delta n_C$ of the finished spun fiber due to manufacturing irregularities and defects. Therefore, the circular birefringence $\Delta n_C$ and the residual linear birefringence $\Delta n_L$ of finished spun fibers should be measured directly and such directly measured data are more desirable for FOCS design engineers to understand the limitations of spun fibers in FOCS systems, for FOCS quality engineers to screening out sub-quality spun fibers, as well as for spun fiber manufacturers to ensure fibers' ultimate quality.

The main objective of our work is to develop a measurement technique capable of accurately measuring the circular and residual linear birefringences of spun fibers which is critical to FOCS applications, especially for meeting the demanding requirement of accuracy on the order of 0.2% or less over the temperature range between –40 °C to + 80 °C [10, 11]. Previous methods for the birefringence measurements include those of using rotating-wave plate and polarizer [12–16], wavelength scanning [17], and the photo-elastic modulators [18, 19]. Such analog techniques relying on using analog signals to obtain birefringences usually have the disadvantages of low repeatability and require complicated methods to compensate for imperfections in the optical components and in moving mechanical parts. Consequently, it is difficult to use them to detect the small variations of $\Delta n_C$ and $\Delta n_L$ in a spun fiber. In our previous publications [20–22], we presented using binary polarization rotators made of magneto-optic crystals for polarization related analysis and achieved exceptionally high accuracy and sensitivity for linear birefringence (differential group delay) measurement of optical fibers, an order of magnitude more sensitive than those relying on the analog techniques. The high accuracy results from the high repeatability of the binary polarization rotators, which enable us to effectively calibrate out the imperfections of the components used in the system. In this paper, we extend our work to simultaneously measure both $\Delta n_C$ and $\Delta n_L$ of the spun fiber by using a similar polarization analysis system. By taking the advantages of the binary nature of the rotators, we measure and decompose the Mueller matrix of a combined fiber made with a length of spun fiber of an unknown circular birefringence splicing onto a length of polarization maintaining (PM) fiber with a known linear birefringence to validate our experimental method and algorithm. We next measure $\Delta n_C$ and $\Delta n_L$ of spun fiber from –40 °C to 80 °C and obtain the values of $\Delta n_C$ and $\Delta n_L$ as a function of temperature T to be $3.34 \times 10^{-5}$-$5.11 \times 10^{-8}$T and $8.1 \times 10^{-6}$-$1.19 \times 10^{-8}$T, respectively. We find, for the first time with the best of authors' knowledge, that $\Delta n_C$ and $\Delta n_L$ are highly linear with the temperature, with a thermal coefficients of $-5.11 \times 10^{-8}$ °C$^{-1}$ and $-1.19 \times 10^{-8}$ °C$^{-1}$, respectively, obtained through curve-fitting, and that the relative changes per °C of the circular and residual linear birefringence are almost identical, with values of –0.152% and –0.147% respectively. We notice that the measured $\Delta n_L$ is more than 10 times larger than that theoretically estimated in an ideal spun fiber. We also find that the bending induced linear

Optics EXPRESS

birefringence resulting from looping the fiber with a diameter of 12 *cm* is about 10 less than $\Delta n_L$ of the spun fiber, consistent with the theoretical predictions [23], which in practice allows reducing the sensing coil down to 12 *cm* in diameter for current sensing applications. We believe that the method and data presented in this paper will be beneficial for making high quality spun fibers, as well as high accuracy fiber optic current sensors.

## 2. Principle

In general, the measured Mueller matrix $M(\lambda)$ of an optical medium, such as a spun fiber, at wavelength $\lambda$ can be decomposed into three Mueller matrices [24–26]:

$$M(\lambda) = M_{\Delta} M_R M_D, \tag{1}$$

where $M_D$ represents a diattenuator which measures the differential loss between the orthogonal polarization eigen states (corresponding to polarization dependent loss, or PDL, commonly used in fiber optics), $M_R$ represents a retarder that measures the differential phase between the two eigen states, and $M_{\Delta}$ represents a depolarizer that characterizes depolarization. Among them, $M_R$ relates to the birefringence characteristics can be separated from $M(\lambda)$ using the method presented in [24]. For the measured fiber, the total retardation is the combined effect of both $\Delta n_L$ and $\Delta n_C$, so the $M_R$ can be decomposed into two matrices: a linear retarder matrix with a linear retardation of $\delta$ and an orientation angle of $\theta$ (the axis of the linear birefrinegnce with respect to the horizontal axis) and a circular retarder matrix with an optical rotation of $\varphi$:

$$M_R = \begin{bmatrix} 1 & 0 & 0 & 0 \\ 0 & \cos^2 2\theta + \sin^2 2\theta \cos\delta & \cos 2\theta \sin 2\theta (1-\cos\delta) & -\sin 2\theta \sin\delta \\ 0 & \cos 2\theta \sin 2\theta (1-\cos\delta) & \sin^2 2\theta + \cos^2 2\theta \cos\delta & \cos 2\theta \sin\delta \\ 0 & \sin 2\theta \sin\delta & -\cos 2\theta \sin\delta & \cos\delta \end{bmatrix} \begin{bmatrix} 1 & 0 & 0 & 0 \\ 0 & \cos 2\varphi & \sin 2\varphi & 0 \\ 0 & -\sin 2\varphi & \cos 2\varphi & 0 \\ 0 & 0 & 0 & 1 \end{bmatrix}. \tag{2}$$

The values of optical rotation $\varphi$ and linear retardation $\delta$ can be determined from the matrix $M_R$ as [24]:

$$\varphi \equiv \frac{\pi L}{\lambda} \Delta n_C = \frac{1}{2} \tan^{-1} \left[ \frac{M_R(3,2) - M_R(2,3)}{M_R(2,2) + M_R(3,3)} \right] + n\pi, \tag{3}$$

$$\delta \equiv \frac{2\pi L}{\lambda} \Delta n_L = \cos^{-1} \left( \left\{ \left[ M_R(2,2) + M_R(3,3) \right]^2 + \left[ M_R(3,2) - M_R(2,3) \right]^2 \right\}^{\frac{1}{2}} - 1 \right) + 2m\pi, \tag{4}$$

where $m$ and $n$ are integers to account for phase wrapping. It is difficult to directly use Eqs. (3) and (4) to calculate $\Delta n_c$ and $\Delta n_L$ at a wavelength $\lambda$ because $m$ and $n$ cannot be determined. In practice, it is beneficial to use a differential method to 1) improve measurement accuracy, and 2) remove the contribution of $m$ and $n$, by first measuring $\varphi$ and $\delta$ at two adjacent wavelengths $\lambda_1$ and $\lambda_2$ and then taking the differences $\Delta\varphi = \varphi(\lambda_1) - \varphi(\lambda_2)$ and $\Delta\delta = \delta(\lambda_1) - \delta(\lambda_2)$, assuming that the wavelength step $\Delta\lambda = \lambda_2 - \lambda_1$ is sufficiently small such that $\Delta\varphi$ and $\Delta\delta$ are less than $\pi$ and $2\pi$, respectively. $\Delta n_c$ and $\Delta n_L$ can then be obtained from the differential rotation angle $\Delta\varphi$ and the differential retardation $\Delta\delta$, respectively, using Eqs. (3) and (4):

$$\Delta n_C = \frac{\lambda_1 \lambda_2}{\pi L (\lambda_2 - \lambda_1)} \Delta\varphi, \tag{5}$$

$$\Delta n_L = \frac{\lambda_1 \lambda_2}{2\pi L (\lambda_2 - \lambda_1)} \Delta\delta. \tag{6}$$

where $\Delta n_c$ and $\Delta n_L$ are assumed constant over wavelength and such an assumption is accurate because of the negligible birefringence dispersion as discussed in Appendix B [29] and the small wavelength step.

Optics EXPRESS

Appendix A shows an example of using the process described above to obtain $\Delta n_C$ and $\Delta n_L$ at 20 °C. To further improve the repeatability and accuracy, the laser frequency can be scanned and the values of $\Delta n_c$ and $\Delta n_L$ can be calculated at multiple such wavelength pairs for averaging.

## 3. Experiment

### *3.1 Experimental setup*

The basic construction of the binary polarization measurement system (PMS) [20] is illustrated in Fig. 1. It consists of a tunable laser, a binary magneto-optic (MO) polarization state generator (PSG), a binary MO polarization analyzer (PSA) and a control computer. The fiber under test is placed between the PSG and PSA. As shown in Fig. 1, the binary PSA and PSG each compose of a quarter-wave plate (QWP), six binary MO polarization rotators and a polarizer. The PSA also contains a photodetector and a signal amplification circuit. In PSG, each binary MO rotator controlled by the computer can rotate the state of polarization (SOP) +/–22.5 degrees to generate 6 distinctive polarization states [22]. The PSA can accurately measure the state of polarization of light entering it by analyzing voltages generated in the photodetector and can also be self-calibrated to remove inaccuracies caused by imperfections in components and workmanship, yielding extremely high measurement accuracies [21]. Collectively, the binary PSG and PSA can be used to accurately obtain the Mueller Matrix of fiber under test [20].

As shown in Fig. 1, in Experiment 1, we first fusion-spliced 1 meter of PM fiber (PM fiber 1550_125-18/250 of YOFC Ltd.) with 10 meters spun fiber (Spun HiBi Fiber SHB1250 (7.3/125) of Fibercore Co. Ltd., with a spin pitch of 4.8 *mm*) to measure $\Delta n_C$ and $\Delta n_L$ to validate our system and algorithm for the birefringence measurement. The two fibers have well matched mode-field diameters of 6.41 $\mu m$ and 6.92 $\mu m$, respectively. In Experiment 2, we put 10 *m* spun fiber in a temperature chamber to measure the relationship between its circular and the residual linear birefringences and temperature using the same binary PSM, as shown in Fig. 1, while having 0.4 *m* of pigtails outside of the chamber. Assuming the circular and linear birefringences are uniform along the spun fiber, we subtract the contributions to the circular and linear birefringences from the 0.4 *m* outside of the chamber during the data processing.

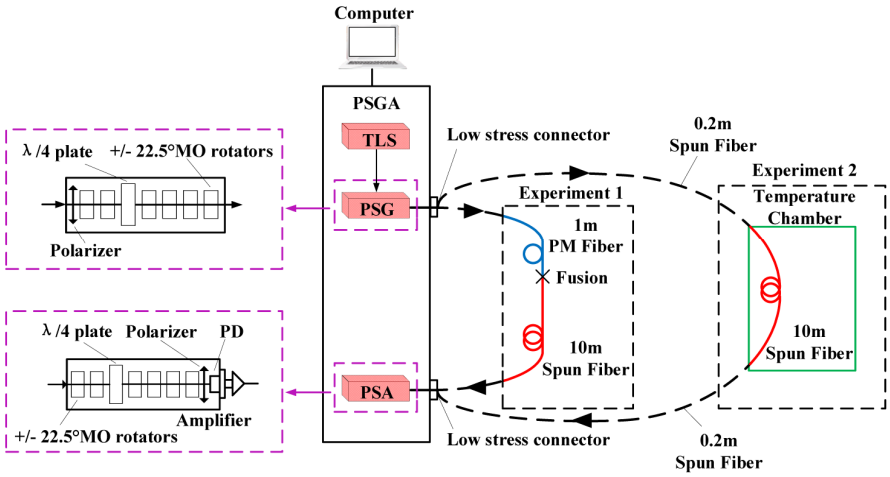


Fig. 1. Experimental setup consisting of a PSG and a PSA made with binary magneto-optic polarization rotators. Light from a tunable laser first goes through a PSG before connecting to a fiber under test (FUT). The FUT is placed between the PSG and PSA to obtain the transfer matrix. In Experiment 1, a known length of PM fiber with a known birefringence is fusion-spliced with a 10 *m* spun fiber for validating our algorithms for $\Delta n_C$ and $\Delta n_L$. In Experiment 2, a continuous length of 10.4 *m* spun fiber was used, in which 10 *m* was put into a temperature

Optics EXPRESS

chamber to obtain the thermal coefficients of both the circular and residual linear birefringences, while the outside 0.4 *m* was used for connecting to the PSG and PSA via low stress connectors.

### 3.2 Verification of birefringence measurements

Our measurement system and algorithm for obtaining accurate linear birefringence using our measurement system has been validated in [20] with artifacts made with quartz crystals having an accurately known linear birefringence. Here we validate our new algorithms for obtaining the circular and the linear birefringences $\Delta n_c$ and $\Delta n_L$ from the measured Muller matrix using Eqs. (2) to (6). We set the wavelength $\lambda 1 = 1549.72$ *nm* and $\lambda 2 = 1550.52$ *nm* with a wavelength spacing of 0.8 *nm* of the internal tunable laser source of PSM. Such a wavelength spacing is sufficiently small to assure $\Delta\varphi < \pi$ and $\Delta\delta < 2\pi$, however, sufficiently large to allow good measurement repeatability and accuracy.

We measure $\Delta n_c$ and $\Delta n_L$ with the following procedures: 1) Fusion-splice 1 meter of polarization-maintaining (PM) fiber with 10 meters of a spun fiber as the fiber under test, as shown in Fig. 1, in which the circular and linear birefringences are assumed to be contributed by the spun fiber and the PM fiber respectively. The linear birefringence $\Delta n_L$ of the PM fiber before splicing is first accurately measured with our system to be $6.63 \times 10^{-4}$ at 1550 *nm*, which is slightly different from $6.59 \times 10^{-4}$ given by the fiber manufacturer. The slight difference may be resulted from different measurement systems or slightly different measurement conditions. We choose to use our measurement value in the paper to ensure the measurement consistency, in addition to our confidence with our measurement system, validated with standard artifacts made with quartz crystals with an exact known birefringence [20]. 2) Obtaining the Mueller matrix using our binary PMS and then calculate $\Delta n_c$ and $\Delta n_L$ with our new algorithms. 3) Cut away 10 *cm* of the PM fiber and repeat step 2 to get a second set of measurement results of $\Delta n_c$ and $\Delta n_L$. 4) Repeat step 3 to get more sets of measurement results of $\Delta n_c$ and $\Delta n_L$. Figure 2 shows the 7 sets of measurement results, corresponding to the cases with 7 different PM fiber lengths from 1 meter down to 0.4 meters. The linear birefringence of the combined fiber can be obtained with our binary system and the new algorithm to be $6.69 \times 10^{-4}$, less than 1% difference from the number obtained using the previously proven algorithm on the PM fiber alone. As expected, the corresponding differential retardation $\Delta\delta$ between two wavelengths of the combined fiber in deed decreases linearly with the length of PM fiber, as shown in Fig. 2(a), with the linear birefringence as the slope of the line. On the other hand, the differential polarization rotation angle $\Delta\varphi$ and the corresponding $\Delta n_c$ of the combined fiber remain almost constant as the PM fiber is being decreased, as shown in Fig. 2(b), indicating that our new algorithm can effectively isolate the influence of the linear birefringence on the measurement of $\Delta n_C$ and vise versa. The obtained $\Delta n_c$ of the combined fiber is $3.47 \times 10^{-5}$ with a standard deviation of $3.28 \times 10^{-7}$, showing again that the linear birefringence of the PM does not affect the measurement of $\Delta n_C$ of the combined fiber. The experiment above therefore validates that our binary system and the new algorithms is capable of simultaneously obtaining the circular and linear birefringences with high accuracies.

Optics EXPRESS

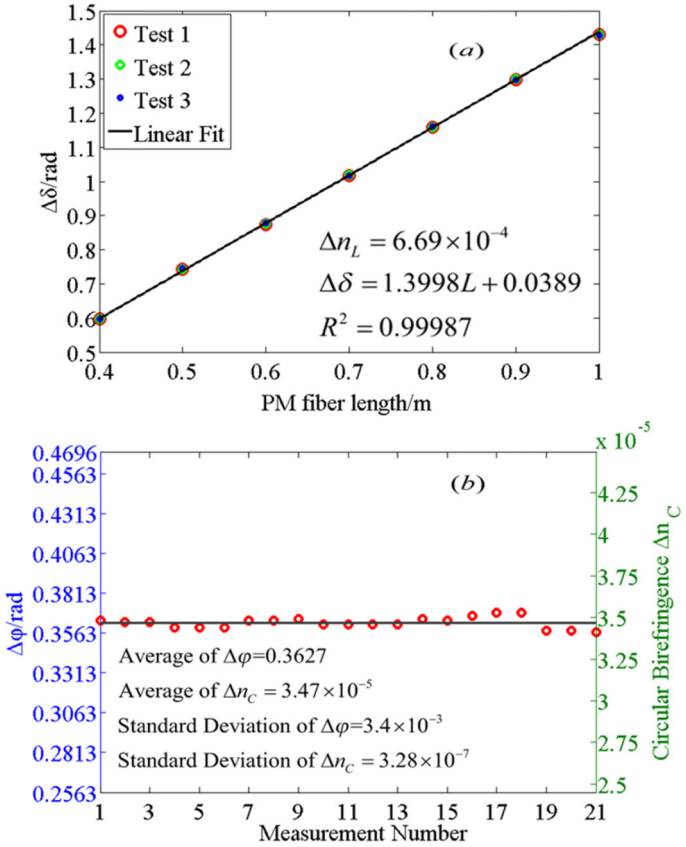


Fig. 2. (a) Experimental results showing that the differential retardation $\Delta\delta$ between two wavelengths decreases as the length of the PM fiber becomes shorter with a linear birefringence $\Delta n_L$ of $6.69 \times 10^{-4}$ representing its slope. (b) Measurement results of differential $\Delta\varphi$ between two wavelengths and the resulting $\Delta n_C$ of a combined fiber of 10 *m* spun fiber with varied lengths of PM fiber. In the experiment, the two wavelengths with a spacing of 0.8 *nm* are set around 1550 *nm* and 3 measurements are taken for each PM fiber length with negligible differences. With 7 different lengths of PM fiber in the combined fiber, the total number of measurements is 21. Because the length of the spun fiber was unchanged, $\Delta\varphi$ should remain constant and be represented by a horizontal line. Therefore the small deviation of the data from the horizontal line indicates the superb repeatability of our measurement.

### *3.3 Thermal coefficient of circular birefringence in spun fiber*

The temperature dependence of $\Delta n_C$ is an important parameter for fiber optic current sensors because it affects the temperature stability of the sensor system and hence its accuracy over temperatures. We put 10 meters of spun fiber coiled with a diameter of 12 *cm* in a temperature chamber and measure $\Delta n_C$ in different temperatures from –40 °C to 80 °C. In our measurements, we scan the wavelength of the tunable laser in our setup from 1528.77 *nm* to 1562.64 *nm*, with a frequency step of *5 × 50 GHz* (~4 *nm*). As described previously, we can obtain the birefringence as a function of wavelength and average the multiple sets of birefringence values as the final values. Figure 3 shows the measurement results of $\Delta n_C$ at seven different temperatures (–40 °C, –20 °C, 0 °C, 20 °C, 40 °C, 60 °C, 80 °C). It is evident that $\Delta n_C$ has a value of $3.24 \times 10^{-5}$ at 20 °C and decreases linearly with the temperature, with a slope of $-5.09 \times 10^{-8}$ °C$^{-1}$, which is the thermal coefficient of circular birefringence $\alpha_C$. It is interesting to note that $\Delta n_c$ of the spun fiber and its thermal coefficient $\alpha_C$ are an order of magnitude less than the linear birefringence $\Delta n_L$ of a PM fiber and its thermal coefficient

Optics EXPRESS

[27], respectively, although the relative change of $\Delta n_c$ of the spun fiber per °C is –0.152%, on the same order of magnitude as that of $\Delta n_L$ of the PM fiber.

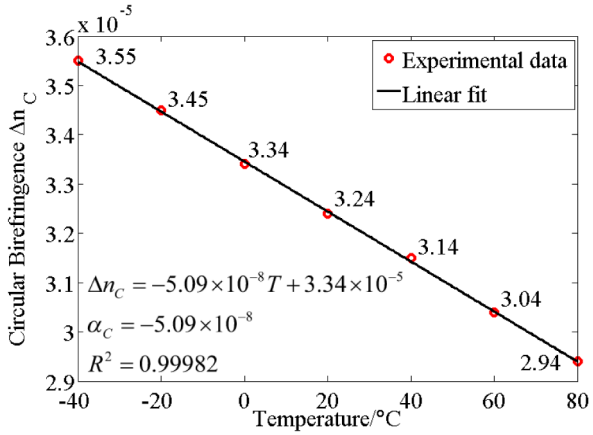


Fig. 3. Measured $\Delta n_C$ of spun fiber at seven different temperatures. Curve fitting yields the thermal coefficient $\alpha_C$ of $\Delta n_C$ to be $-5.09 \times 10^{-8}$ °C$^{-1}$. The relative change of $\Delta n_C$ per °C, defined as the ratio of $\alpha_C$ and $\Delta n_C$ at T = 0, is –0.152%.

To obtain the repeatability of the measurement, we performed nine repeated measurements and the resultsare shown in Fig. 4. The average thermal coefficient $\alpha_C$ of nine measurements is $-5.11 \times 10^{-8}$ °C$^{-1}$ and the standard deviation of the nine measurements is $3.48 \times 10^{-10}$, which represents less than 1% of measurement fluctuations and demonstrates the superb resolution and accuracy of our binary polarization measurement system.

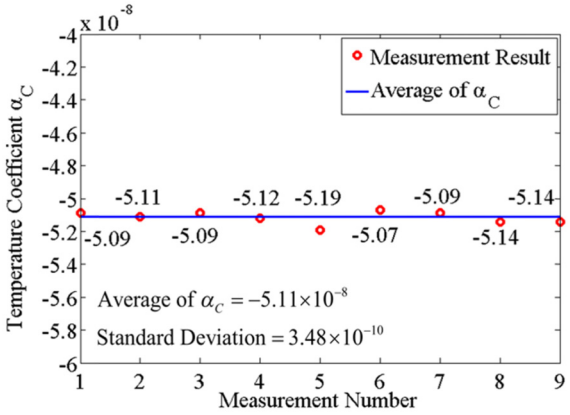


Fig. 4. Repeatability measurements of the thermal coefficient of circular birefringence $\alpha_C$ of a spun fiber under test, with an average of $-5.11 \times 10^{-8}$° C$^{-1}$ and a standard deviation of $3.48 \times 10^{-10}$ C$^{-1}$.

### *3.4 Linear birefringence measurement in spun fiber with different temperatures*

In the fabrication of a spun fiber, spinning a fiber with a strong linear birefringence will make the fiber having a strong circular birefringence but greatly reduces its intrinsic linear birefringence [4]. For current sensing applications, we hope $\Delta n_L$ has a relatively small value that can ensure the accuracy of FOCS and withstand external disturbances. Therefore, it is important to accurately determine $\Delta n_L$ of a spun fiber and its temperature dependence.

While measuring $\Delta n_C$ of the 10 meters spun fiber, we also obtain its $\Delta n_L$ in different temperatures, with the results shown in Fig. 5. As mentioned previously, the spun fiber was

Optics EXPRESS

coiled with a diameter of 12 *cm* and was put in a temperature chamber. Totally 3 sets of measurements labeled Test 1, Test 2, and Test 3 were performed at seven temperatures from –40 °C to 80 °C and the measurements at each temperature were repeated 3 times. After each set of measurements, the coiled spun fiber in the chamber was purposely re-arranged and re-connected with the measurement system to alter the polarization states inside the fiber. The data fluctuation at each temperature in each test set is represented by an error bar. As one can see from Fig. 5 that the 3 measurements at each temperature in each test set is highly repeatable, however, the data at each temperature in different test sets have relatively large fluctuations. Nevertheless, it is evident from Fig. 5 that $\Delta n_L$ of the spun fiber is around $7.80 \times 10^{-6}$ (about 4 times smaller than its circular birefringence) at room temperature (20 °C) and also decreases with temperature. In Fig. 5, we averaged nine sets of data at each temperature and made a linear fit of the value. The slope of the linear fit is $-1.19 \times 10^{-8}$ °C$^{-1}$, which is the thermal coefficient $\alpha_L$ of $\Delta n_L$. It is interesting and important to notice that the relative change of $\Delta n_L$ per °C of the spun fiber is –0.147%, almost identical to the relative change of $\Delta n_c$ per °C of –0.152%, despite the large difference between the thermal coefficients of the circular and linear birefringences $\Delta n_c$ and $\Delta n_L$. It is also interesting to notice that the temperature dependence of a PANDA PM fiber's birefringence is $6.22 \times 10^{-4} - 5.93 \times 10^{-7}$T [27] and the relative change per °C is –0.095%, also on the same order of magnitude as the relative change of the spun fiber's $\Delta n_c$ and $\Delta n_L$ per °C, suggesting that these temperature dependences may all be caused by the anisotropic strain resulting from the differential thermal expansions between the stress rods and the rest of the fiber cladding [27, 28]. However, such expectations must be further studied to be conclusive.

To verify the repeatability of our measurement, just as circular birefringence measurements, we also performed nine repeated measurements and the resultsin Fig. 6. The average thermal coefficient $\alpha_L$ of nine measurements is $-1.20 \times 10^{-8}$ °C$^{-1}$ and the standard deviation of nine measurements is $7.40 \times 10^{-9}$.

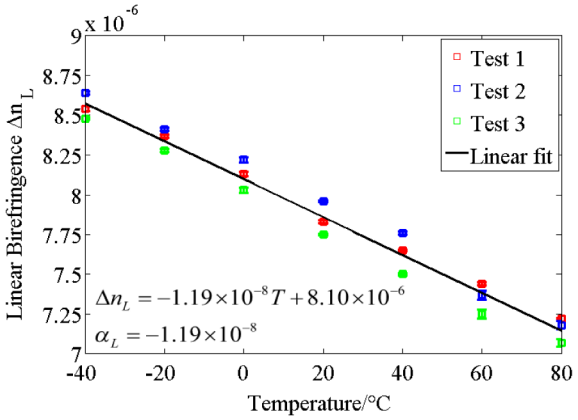


Fig. 5. Measured $\Delta n_L$ of 10 *m* spun fiber at seven different temperatures. We firstly measure the $\Delta n_L$ in a stable external condition for three times at each temperature points and give out the error bar chart. Then gave a tiny external disturb to the fiber coils and measured repeatedly for three groups. We averaged nine sets of data at the same temperature and made the linear fit, the slope of the fitting line represents the thermal coefficient $\alpha_L$ of residual linear birefringence that is $-1.19 \times 10^{-8}$ °C$^{-1}$. The relative change per °C, defined as the ratio of $\alpha_L$ and $\Delta n_L$ at T = 0, is –0.147%.

Optics EXPRESS

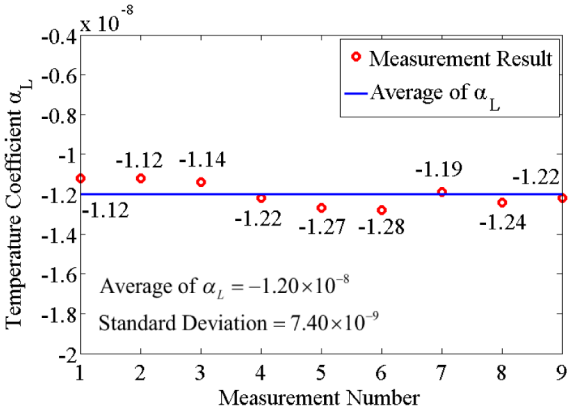


Fig. 6. Repeatability measurements of the thermal coefficient of residual linear birefringence $\alpha_L$ of a spun fiber under test

Note that the bending induced birefringence in a coiled fiber of 12 *cm* diameter from [23] is 5.34 × $10^{-7}$. We experimentally confirmed such bending induced linear birefringence to be 6.10 × $10^{-7}$ by measuring a length of single mode fiber coiled with a diameter of 12 *cm* using our binary polarization measurement system. Such a bending induced birefringence is an order of magnitude smaller than the residual linear birefringence of the spun fiber and is expected to have negligible effect on the accuracy of the spun fiber measurement. These experimental results also indicate that the current sensing coils may also be coiled down to a diameter on the order of 12 *cm* with negligible impact on the temperature stability of the current sensing system.

Also note that the theoretical results of the spun fiber calculated using the theory in [1,4] with the parameters specified in manufacturer's data sheet are between 1.05 × $10^{-5}$-2.08 × $10^{-5}$ for $\Delta n_C$ and less than 2.62 × $10^{-7}$ for the residual linear birefringence $\Delta n_L$ at 1310 *nm*, as shown in Appendix B. The corresponding $\Delta n_C$ and $\Delta n_L$ at 1550 *nm* are estimated to be 8.83 × $10^{-6}$ –1.76 × $10^{-5}$ and 3.1 × $10^{-7}$, respectively, from Appendix B. They are significantly different from the measured values of 3.24 × $10^{-5}$ for $\Delta n_C$ and 7.80x$10^{-6}$ for $\Delta n_L$ at 20 °C at 1550 *nm*, validating our concerns that the irregularities and imperfections in the manufacturing process causes the actual birefringence values to significantly deviate from the designed values, and re-affirming our suggestion that accurate measurement method and results are necessary for the users of spun fibers for current sensing and other demanding applications, especially considering that the residual linear birefringence $\Delta n_L$ of a real spun fiber is more than 10 times larger than that of an ideal spun fiber.

## 4. Summary

In summary, we present a method to accurately measure the birefringence of a spun fiber using a polarization analysis system with binary polarization rotators. By taking the advantages of high accuracy and high resolution of the binary system, we accurately measure the circular birefringence $\Delta n_C$ and residual linear birefringence $\Delta n_L$ of the spun fiber as a function of temperature. We first validate our system and algorithm by using a combined fiber of a fixed length spun fiber and variable lengths of PM fiber of known linear birefringence. We next obtain circular birefringence of the spun fiber to be $\Delta n_C$ = 3.34 × $10^{-5}$-5.11 × $10^{-8}$T, in the temperature range of –40 °C to 80 °C, with a measurement repeatability of less than 1%. Finally, we obtain the residual linear birefringence of the spun fiber as a function of temperature from –40 °C to 80 °C is $\Delta n_L$ = 8.1 × $10^{-6}$-1.19 × $10^{-8}$ T, which is about 4 times less than $\Delta n_C$ of the same fiber, however, more than 10 times larger than the residual linear birefringence theoretically predicted for an ideal spun fiber. We find that the

Optics EXPRESS

relative changes per °C of the circular and residual linear birefringence are almost identical, with values of –0.152% and –0.147% respectively. It should be pointed out that a spun fiber's thermal coefficients of circular birefringence $\alpha_C = -5.11 \times 10^{-8}$ °C$^{-1}$ and residual linear birefringence $\alpha_L = -1.19 \times 10^{-8}$°C$^{-1}$ are the first time reported to the best of authors' knowledge. We believe that the method and experimental results presented in this paper are beneficial for applications in fiber optic current sensing and other demanding applications.

Further studies are required to investigate the origins of the temperature dependences of the circular and residual linear birefringences of the spun fiber, as well as their dependence on other parameters, such as the spinning pitch during fiber drawing.

## 5. Appendix A

The measured 4×4 Mueller matrix M($\lambda$) of the 10.4 *m* spun fiber at 20 °C and its decompositions, the diattenuator $M_D$, the retarder $M_R$, and the depolarizer $M_\Delta$, at $\lambda_1$=1549.72 *nm* and $\lambda_2$=1550.52 *nm* with a sufficiently small wavelength step of 0.8 *nm*, are shown in Tables 1 and 2 below:

**Table 1. Measured Mueller matrix and its decompositions of the 10.4 *m* spun fiber (20°C, $\lambda_1$ = 1549.72 *nm*)**

| $M$ | $M_\Delta$ |
|---|---|
| $\begin{pmatrix} 1.0000 & 0.0010 & 0.0000 & -0.0020 \\ 0.0100 & 0.7010 & 0.5200 & 0.5270 \\ -0.0070 & -0.0140 & -0.7350 & 0.6740 \\ 0.0090 & 0.7140 & -0.4530 & -0.5490 \end{pmatrix}$ | $\begin{pmatrix} 1.0000 & 0.0000 & 0.0000 & 0.0000 \\ 0.0104 & 1.0193 & -0.0184 & -0.0122 \\ -0.0056 & -0.0184 & 0.9969 & -0.0236 \\ 0.0072 & -0.0122 & -0.0236 & 1.0078 \end{pmatrix}$ |
| $M_R$ | $M_D$ |
| $\begin{pmatrix} 1.0000 & 0.0000 & 0.0000 & 0.0000 \\ 0.0000 & 0.6966 & 0.4913 & 0.5229 \\ 0.0000 & 0.0158 & -0.7391 & 0.6734 \\ 0.0000 & 0.7173 & -0.4608 & -0.5226 \end{pmatrix}$ | $\begin{pmatrix} 1.0000 & 0.0010 & 0.0000 & -0.0020 \\ 0.0010 & 1.0000 & 0.0000 & 0.0000 \\ 0.0000 & 0.0000 & 1.0000 & 0.0000 \\ -0.0020 & 0.0000 & 0.0000 & 1.0000 \end{pmatrix}$ |

**Table 2. Measured Mueller matrix and its decompositions of the 10.4 *m* spun fiber (20°C, $\lambda_2$ = 1550.52 *nm*)**

| $M$ | $M_\Delta$ |
|---|---|
| $\begin{pmatrix} 1.0000 & 0.0030 & 0.0030 & -0.0030 \\ -0.0020 & 0.1540 & -0.3230 & 0.7200 \\ -0.0090 & -0.8130 & -0.5610 & -0.1240 \\ 0.0040 & 0.5660 & -0.6990 & -0.2980 \end{pmatrix}$ | $\begin{pmatrix} 1.0000 & 0.0000 & 0.0000 & 0.0000 \\ 0.0007 & 0.8019 & -0.0180 & 0.0561 \\ -0.0053 & -0.0180 & 0.9952 & -0.0155 \\ 0.0035 & 0.0561 & -0.0155 & 0.9457 \end{pmatrix}$ |
| $M_R$ | $M_D$ |
| $\begin{pmatrix} 1.0000 & 0.0000 & 0.0000 & 0.0000 \\ 0.0000 & 0.1335 & -0.3650 & 0.9214 \\ 0.0000 & -0.8055 & -0.5816 & -0.1137 \\ 0.0000 & 0.5774 & -0.7270 & -0.3717 \end{pmatrix}$ | $\begin{pmatrix} 1.0000 & 0.0030 & 0.0030 & -0.0030 \\ 0.0030 & 1.0000 & 0.0000 & 0.0000 \\ 0.0030 & 0.0000 & 1.0000 & 0.0000 \\ -0.0030 & 0.0000 & 0.0000 & 1.0000 \end{pmatrix}$ |

The values of $\delta$ and $\varphi$ at the two wavelengths $\lambda_1$ and $\lambda_2$ can be obtained to be $\delta(\lambda_1) = (2m\pi + 2.1207)$ *rad*, $\delta(\lambda_2) = (2m\pi + 1.9516)$ *rad*, $\varphi(\lambda_1) = (n\pi + 0.7408)$ *rad*, and $\varphi(\lambda_2) = (n\pi + 0.3884)$ *rad*, respectively, using Eq. (3), Eq. (4) and the matrix $M_R$ at the corresponding wavelength. Finally, the residual linear birefringence $\Delta n_L$ and the circular birefringence $\Delta n_C$ of the 10.4 *m* spun fiber at 20°C can be obtained to be $\Delta n_L = 7.77 \times 10^{-6}$ and $\Delta n_C = 3.24 \times 10^{-5}$ using Eqs. (5) and (6).

Optics EXPRESS

## 6. Appendix B

Theoretical calculation of spun fiber's circular birefringence and residual linear birefringence from [1,4], the relationship among the spin pitch $L_t$, the elliptical beat length $L_c$, and the linear beat length $L_p$ of the equivalent unspun fiber with the same perform can be expressed as:

$$L_p = \left( \frac{1}{L_c^{\,2}} + \frac{4}{L_t \cdot L_c} \right)^{-\frac{1}{2}}, \tag{7}$$

where $L_p = \lambda/\Delta n_l$ and $\Delta n_l$ is the linear birefringence of the equivalent un-spun HiBi fiber. The linear retardance $\delta(L)$ and optical rotation $\varphi(L)$ of a spun fiber of length $L$ can be expressed as [1]:

$$\delta(L) = 2\sin^{-1}\left( \frac{1}{\left(1+(2\xi/\Delta\beta)^2\right)^{1/2}} \cdot \sin\frac{\sqrt{\Delta\beta^2+4\xi^2}}{2} L \right), \tag{8}$$

$$\varphi(L) = \xi L + \tan^{-1}\left( \frac{-(2\xi/\Delta\beta)}{\left(1+(2\xi/\Delta\beta)^2\right)^{1/2}} \cdot \tan\frac{\sqrt{\Delta\beta^2+4\xi^2}}{2} L \right) + k\pi, \tag{9}$$

where $\Delta\beta = 2\pi/L_p$, $\xi = 2\pi/L_t$, and $k$ is an integer.

We first estimate the circular birefringence and the residual linear birefringence at 1310 *nm*. From spun fiber's data sheet [9], the spin pitch $L_t$ = 4.8 *mm* and the elliptical beat length $L_c$ = 63-125 *mm at 1310 nm*, the linear beat length of the unspun fiber $L_p$ can be estimated to be 8.62-12.2 *mm* using Eq. (7), $\Delta\beta$ and $\xi$ can be obtained to be 515-729 *rad/m* and 1309 *rad/m*, respectively. The corresponding linear birefringence of the equivalent unspun HiBi fiber is between $1.07\times10^{-4}$ and $1.52\times10^{-4}$ at 1310 *nm*. The value of $\delta(L)$ then can be obtained using Eq. (8) and finally $\Delta n_L$ can be obtained with the maximum value of $2.62\times10^{-7}$ using $\delta=2\pi L\Delta n_L/\lambda$, when the fiber length $L$ of 10 *m* is used. Similarly, the $\varphi(L)$ of a 10 *m* spun fiber can be obtained by using Eq. (9) between 250-498 *rad.* Consequently, the theoretical value of $\Delta n_C$ is between $1.04\times10^{-5}$-$2.08\times10^{-5}$ at 1310 *nm* using $\varphi = \pi L\Delta n_C/\lambda$.

We next estimate the circular birefringence and the residual linear birefringence at 1550 *nm* because our measurements of the spun fiber are performed at 1550 *nm*, not 1310 *nm*. The birefringence dispersion [29] may contribute a difference to the birefringence at 1550 *nm* from the value at 1310 *nm* for a linear polarization maintaining fiber. However, such a contribution is on the order of 0.122% if the birefringence dispersion of 0.0079 *ps/(km·nm)* is used [29], and is negligible so that the linear birefringence value, $1.071\times10^{-4}$ - $1.522\times10^{-4}$, of the equivalent unspun HiBi fiber at 1310 *nm* can be used for 1550 *nm.* Therefore, the linear beat length $L_p$ at 1550 *nm* and the corresponding value of $\Delta\beta$ can be estimated to be 10.20-14.49 *mm* and 434-616 *rad/m*, respectively. With the known value $\xi$ of 1309 *rad/m*, the residual linear birefringence $\Delta n_L$ of the spun fiber is estimated to be less than $3.1\times10^{-7}$ using Eq. (8) and $\delta=2\pi L\Delta n_L/\lambda$ and its circular $\Delta n_C$ can be estimated to be $8.83\times10^{-6}$ –$1.76\times10^{-5}$ using Eq. (9) and $\varphi = \pi L\Delta n_C/\lambda$ at 1550 *nm*, respectively.

## Funding

National Natural Science Foundation of China (Grant Nos. 61505138, 61635008), Tianjin Science and Technology Support Plan Program Funding (Grant No.16JCQNJC01800), China Postdoctoral Science Foundation (Grant No.2015M580199, 2016T90205), National Instrumentation Program (Grant No. 2013YQ030915), National key research and development programs (Grant Nos. 2016YFC0100500, 2016YFF0102407), International

Optics EXPRESS

Science & Technology Cooperation Program of China (Grant No. 2014DFA12930), and internal development funding of General Photonics Corporation.

## Acknowledgments

We thank Lailong Wang and Yanling Shang of the Photonics Information Innovation Center of Hebei University for helping to take measurement data, Di Yang, Haihao Dong, Jing Li of Tianjin University for helpful discussions, and Dr. Chris Emslie of Fibercore for providing the spun fiber.